ISTITUTO NAZIONALE DI FISICA NUCLEARE
Laboratori Nazionali di Frascati

LNF-84/2

M.Basile et al.: UNIVERSALITY FEATURES IN (pp), (e^+e^-) AND DEEP-INELASTIC-SCATTERING PROCESSES

Estratto da:
Nuovo Cimento 79A, 1 (1984)

Servizio Documentazione
dei Laboratori Nazionali di Frascati
Cas. Postale 13 - Frascati (Roma)

IL NUOVO CIMENTO VOL. 79 A, N. 1 1 Gennaio 1984

Universality Features in (pp), (e^+e^-) and Deep-Inelastic-Scattering Processes.

M. BASILE, G. BONVICINI, G. CARA ROMEO, L. CIFARELLI, A. CONTIN
M. CURATOLO, G. D'ALÍ, C. DEL PAPA, B. ESPOSITO, P. GIUSTI, T. MASSAM
R. NANIA, F. PALMONARI, G. SARTORELLI, G. SUSINNO, L. VOTANO
and A. ZICHICHI

CERN - Geneva, Switzerland
Istituto di Fisica dell'Università - Bologna, Italia
Istituto Nazionale di Fisica Nucleare, Laboratori Nazionali di Frascati - Frascati, Italia
Istituto Nazionale di Fisica Nucleare - Sezione di Bologna, Italia

(ricevuto il 29 Luglio 1983)

Summary. — The use of the correct variables in (pp), (e^+e^-), and deep-inelastic scattering (DIS) processes allows universality features to be established in these—so far considered—different ways of producing multihadronic states.

PACS. 25.30. – Lepton-induced reactions and scattering.
PACS. 25.40. – Nuclear-induced reactions and scattering.

1. – Introduction.

Multihadronic final states can be produced in purely hadronic interactions such as (pp), in purely electromagnetic interactions such as (e^+e^-), and in lepton-hadron deep-inelastic-scattering (DIS) processes, which can be either weak (such as νp) or electromagnetic (such as μp).

The purpose of this paper is to review the main points needed in order to establish a common basis for a comparison between these various ways of producing multihadronic states. The interest in this study is twofold:

i) So far, these three ways of producing multiparticle systems have been considered to be basically different. Our study shows that, before reaching

such a conclusion, it is imperative to use the correct variables in describing the three processes: (pp), (e^+e^-) and DIS. In fact, the use of the correct variables allows universal features to be revealed in the multihadronic final states produced in (pp), (e^+e^-) and DIS.

ii) Once these—so far considered—different ways of producing multihadronic final states are brought within the correct framework, the comparison can be made at a deeper level, and basic differences can thus be studied, if they exist. These differences must be at a level which is below our present one, where we have established striking common features.

We will see that (pp) interactions can be studied *à la* (e^+e^-) and *à la* DIS. However, the DIS way turns out to be incorrect when comparing DIS data with those obtained in (e^+e^-). The equivalence found between (pp) and (e^+e^-) data allows the « differences » reported between DIS and (e^+e^-) data to be understood. These differences are reproduced if (pp) data are analysed *à la* DIS, and disappear when the correct variables are used.

In sect. **2** we introduce the correct variables. In sect. **3** we report all results obtained so far when comparing (pp), (e^+e^-) and DIS. In sect. **4** we extrapolate our findings to the multihadronic systems to be studied at collider energies, such as at the CERN ($p\bar{p}$) machine. Section **5** gives the conclusions.

Notice that the universality features discovered are a zero-parameter fit to the various properties of the multihadronic systems produced in (pp), (e^+e^-), and DIS.

2. – The identification of the correct variables.

The identification of the correct variables for describing hadron production in (pp) interactions, (e^+e^-) annihilation and DIS processes is the basic starting point for putting these three ways of producing multiparticle hadronic systems on an equal footing. In this section we show how this can be done.

2·1. – e^+e^- *annihilation* is illustrated in fig. 1, where $q_1^{\rm inc}$ and $q_2^{\rm inc}$ are the four-momenta of the incident electron e^- and positron e^+; $q^{\rm h}$ is the four-momentum of a hadron produced in the final state, whose total energy is

$$(\sqrt{s})_{e^+e^-} = \sqrt{(q_1^{\rm inc} + q_2^{\rm inc})^2} = 2E_{\rm beam} \tag{1}$$

(when the colliding beams have the same energy).

As we will see later,

$$q_1^{\rm inc} = q_1^{\rm had}, \qquad q_2^{\rm inc} = q_2^{\rm had}, \tag{2}$$

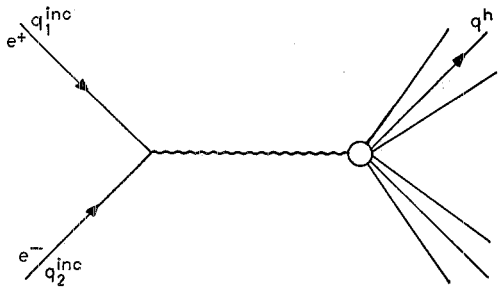

Fig. 1. – Schematic diagram for the (e^+e^-) annihilation.

where $q_{1,2}^{had}$ are the four-momenta available in a (pp) collision for the production of a final state with total hadronic energy

$$\sqrt{(q_1^{had} + q_2^{had})^2} = \sqrt{(q_{tot}^{had})^2}. \tag{3}$$

It is this quantity $\sqrt{(q_{tot}^{had})^2}$ which should be used in the comparison with (e^+e^-) annihilation, and therefore with

$$(\sqrt{s})_{e^+e^-}. \tag{4}$$

This means that

$$(\sqrt{s})_{e^+e^-} = \sqrt{(q_{tot}^{had})^2}. \tag{5}$$

Moreover, the fractional energy of a hadron produced in the final state of an (e^+e^-) annihilation is given by

$$(x)_{e^+e^-} = 2\,\frac{q^h \cdot q_{tot}^{had}}{q_{tot}^{had} \cdot q_{tot}^{had}} = 2\,\frac{E^h}{(\sqrt{s})_{e^+e^-}}, \tag{6}$$

where the dots indicate the scalar product and E^h is the energy of the hadron « h » measured in the (e^+e^-) c.m. system, where that the four-momentum q_{tot}^{had} has no spacelike part:

$$q_{tot}^{had} \equiv [i\mathbf{0}; (\sqrt{s})_{e^+e^-}]. \tag{7}$$

2·2. – DIS *processes* are illustrated in fig. 2, where q_1^{inc} and $q_1^{leading}$ are the four-momenta of the initial- and final-state leptons, respectively; q_2^{inc} is the four-

momentum of the target nucleon; q_1^{had} is the four-momentum transferred from the leptonic to the hadronic vertex, whose timelike component in the laboratory reference system is coincident with the invariant quantity, usually indicated as ν:

$$q_1^{\mathrm{had}} \equiv (i\boldsymbol{p}_1^{\mathrm{had}};\ \nu \equiv E_1^{\mathrm{had}})\,. \tag{8}$$

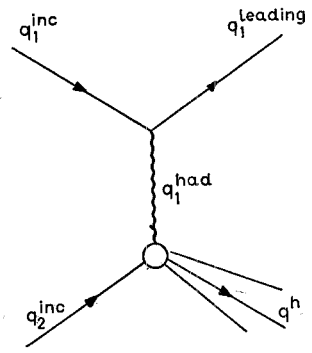

Fig. 2. – Schematic diagram for the DIS processes.

Notice that, in order to easily identify the equivalent variables in (pp) interactions, we have introduced a notation in terms of E_1^{had} and $\boldsymbol{p}_1^{\mathrm{had}}$.

A basic quantity in DIS is the total hadronic mass

$$(W^2)_{\mathrm{DIS}} = (q_1^{\mathrm{had}} + q_2^{\mathrm{inc}})^2\,, \tag{9}$$

and the fractional energy is

$$(z)_{\mathrm{DIS}} = \frac{q^{\mathrm{h}} \cdot q_2^{\mathrm{inc}}}{q_1^{\mathrm{had}} \cdot q_2^{\mathrm{inc}}}\,, \tag{10}$$

where again the dots between the four-momenta indicate their scalar product.

2·3. – (pp) *interactions* are illustrated in fig. 3, where $q_{1,2}^{\mathrm{inc}}$ are the four-momenta of the two incident protons, $q_{1,2}^{\mathrm{leading}}$ are the four-momenta of the two leading protons, $q_{1,2}^{\mathrm{had}}$ are the spacelike four-momenta emitted by the two proton vertices, q^{h} is the four-momentum of a hadron produced in the final state.

Now, attention! A (pp) collision can be analysed in such a way as to produce the key quantities proper to (e^+e^-) annihilation and DIS processes.

In fact, from fig. 3 we can work out the following quantities, which are

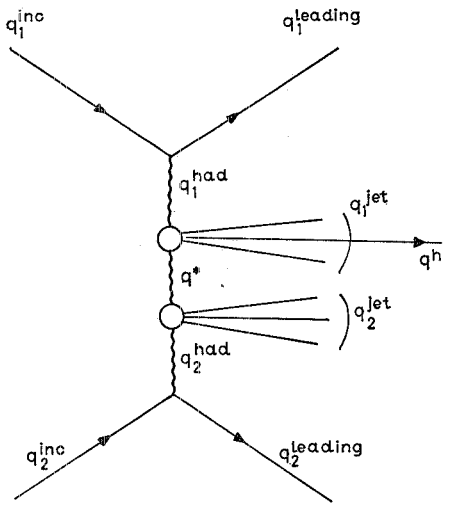

Fig. 3. – Schematic diagram for the (pp) interactions.

needed if we want to compare (pp) physics with (e^+e^-), *i.e.*

$$(q_{tot}^{had})_{pp} = q_1^{inc} + q_2^{inc} - q_1^{leading} - q_2^{leading} = (q_1^{had} + q_2^{had})_{pp}; \tag{11}$$

and (see formula (5))

$$\sqrt{(q_{tot}^{had})_{pp}^2} = (\sqrt{s})_{e^+e^-}. \tag{12}$$

Moreover,

$$(x)_{pp}^{had} = 2\,\frac{q^h \cdot q_{tot}^{had}}{q_{tot}^{had} \cdot q_{tot}^{had}}, \tag{13}$$

to be compared with

$$(x)_{e^+e^-}^{had} = 2\,\frac{q^h \cdot (q_{tot}^{had})_{e^+e^-}}{(q_{tot}^{had})_{e^+e^-} \cdot (q_{tot}^{had})_{e^+e^-}}. \tag{14}$$

The subscripts (e^+e^-) in formula (14) are there to make it clear that these quantities are measured in (e^+e^-) collisions and are the quantities equivalent to those measured in (pp) interactions.

The same (pp) diagram (fig. 3) can be used to work out the key quantities

needed when we want to compare (pp) physics with DIS. In this case we have

$$(W^2)_{pp}^{had} = (q_1^{had} + q_2^{inc})^2 \tag{15}$$

and

$$(z)_{pp}^{had} = \frac{q^h \cdot q_2^{inc}}{q_1^{had} \cdot q_2^{inc}}. \tag{16}$$

Note that in W^2 the leading proton No. 2 is not subtracted. This is the reason for the differences found in the comparison between DIS data and e^+e^- (see sect. **3** and ref. ([15])). In fact W^2 is not the effective total energy available for particle production, owing to the presence there of the leading proton.

3. – Experimental results.

A series of experimental results, where (pp) interactions have been analysed *à la* e^+e^- and *à la* DIS, have given impressive analogies in the multiparticle systems produced in these—so far considered—basically different processes: (pp), (e^+e^-), DIS.

The experimental data in which (pp) interactions are compared with (e^+e^-) are shown in fig. 4-18 and ref. ([1-14]).

([1]) M. BASILE, G. CARA ROMEO, L. CIFARELLI, A. CONTIN, G. D'ALÍ, P. DI CESARE, B. ESPOSITO, P. GIUSTI, T. MASSAM, F. PALMONARI, G. SARTORELLI, G. VALENTI and A. ZICHICHI: *Phys. Lett. B*, **92**, 367 (1980).

([2]) M. BASILE, G. CARA ROMEO, L. CIFARELLI, A. CONTIN, G. D'ALÍ, P. DI CESARE, B. ESPOSITO, P. GIUSTI, T. MASSAM, R. NANIA, F. PALMONARI, G. SARTORELLI, G. VALENTI and A. ZICHICHI: *Nuovo Cimento A*, **58**, 193 (1980).

([3]) M. BASILE, G. CARA ROMEO, L. CIFARELLI, A. CONTIN, G. D'ALÍ, P. DI CESARE, B. ESPOSITO, P. GIUSTI, T. MASSAM, R. NANIA, F. PALMONARI, G. SARTORELLI, G. VALENTI and A. ZICHICHI: *Phys. Lett. B*, **95**, 311 (1980).

([4]) M. BASILE, G. CARA ROMEO, L. CIFARELLI, A. CONTIN, G. D'ALÍ, P. DI CESARE, B. ESPOSITO, P. GIUSTI, T. MASSAM, R. NANIA, F. PALMONARI, G. SARTORELLI, G. VALENTI and A. ZICHICHI: *Lett. Nuovo Cimento*, **29**, 491 (1980).

([5]) M. BASILE, G. CARA ROMEO, L. CIFARELLI, A. CONTIN, G. D'ALÍ, P. DI CESARE, B. ESPOSITO, P. GIUSTI, T. MASSAM, R. NANIA, F. PALMONARI, G. SARTORELLI, M. SPINETTI, G. SUSINNO, G. VALENTI and A. ZICHICHI: *Phys. Lett. B*, **99**, 247 (1981).

([6]) M. BASILE, G. CARA ROMEO, L. CIFARELLI, A. CONTIN, G. D'ALÍ, P. DI CESARE, B. ESPOSITO, P. GIUSTI, T. MASSAM, R. NANIA, F. PALMONARI, G. SARTORELLI, M. SPINETTI, G. SUSINNO, G. VALENTI and A. ZICHICHI: *Lett. Nuovo Cimento*, **30**, 389 (1981).

([7]) M. BASILE, G. CARA ROMEO, L. CIFARELLI, A. CONTIN, G. D'ALÍ, P. DI CESARE,

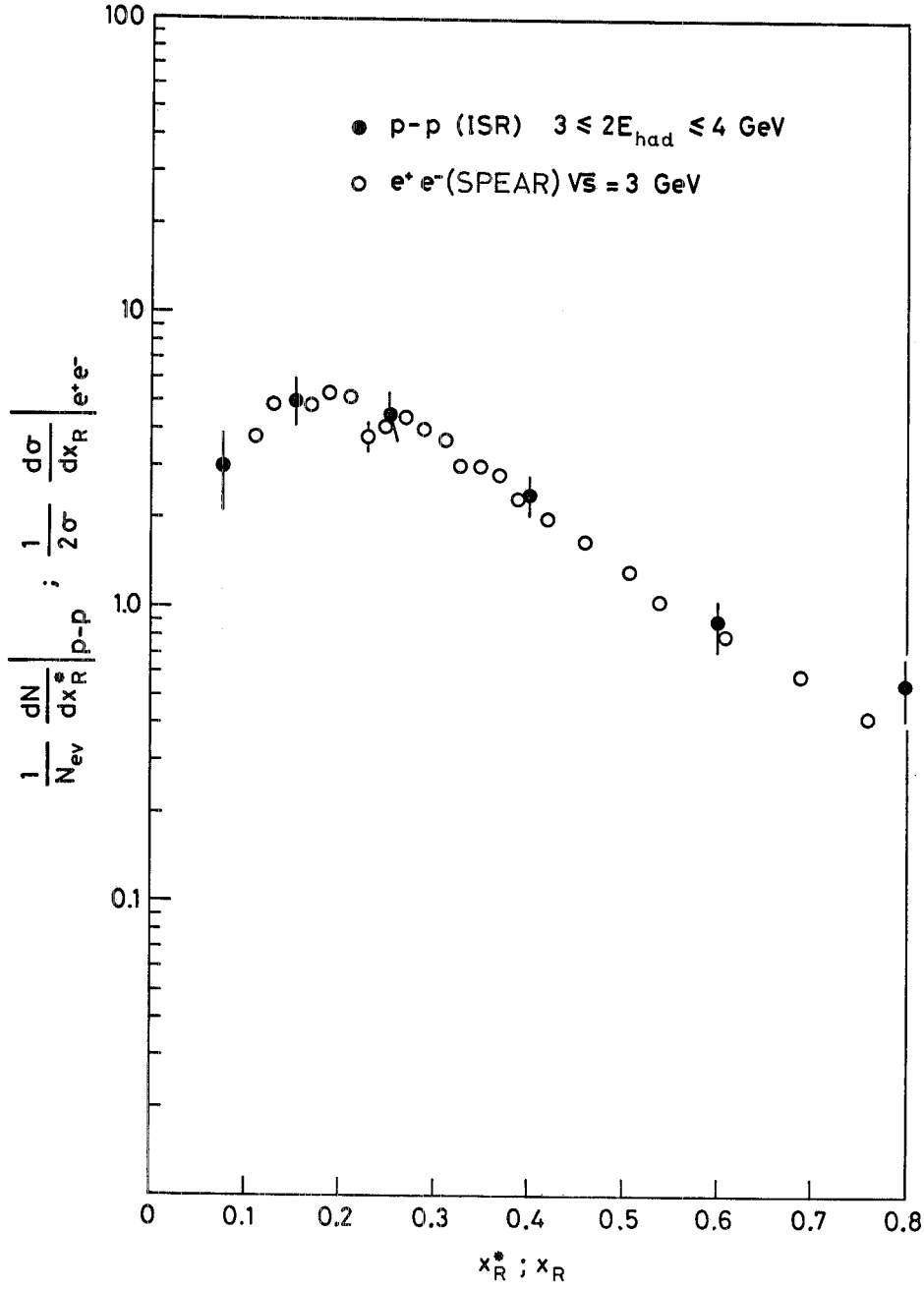

Fig. 4. – The inclusive single-particle fractional momentum distributions $(1/N_{ev})\cdot(dN/dx_R^*)$ in the interval $3\ \mathrm{GeV} \leqslant 2E^{had} \leqslant 4\ \mathrm{GeV}$ obtained from data at $\sqrt{s} = 30$ GeV. Also shown are data from MARK I at SPEAR.

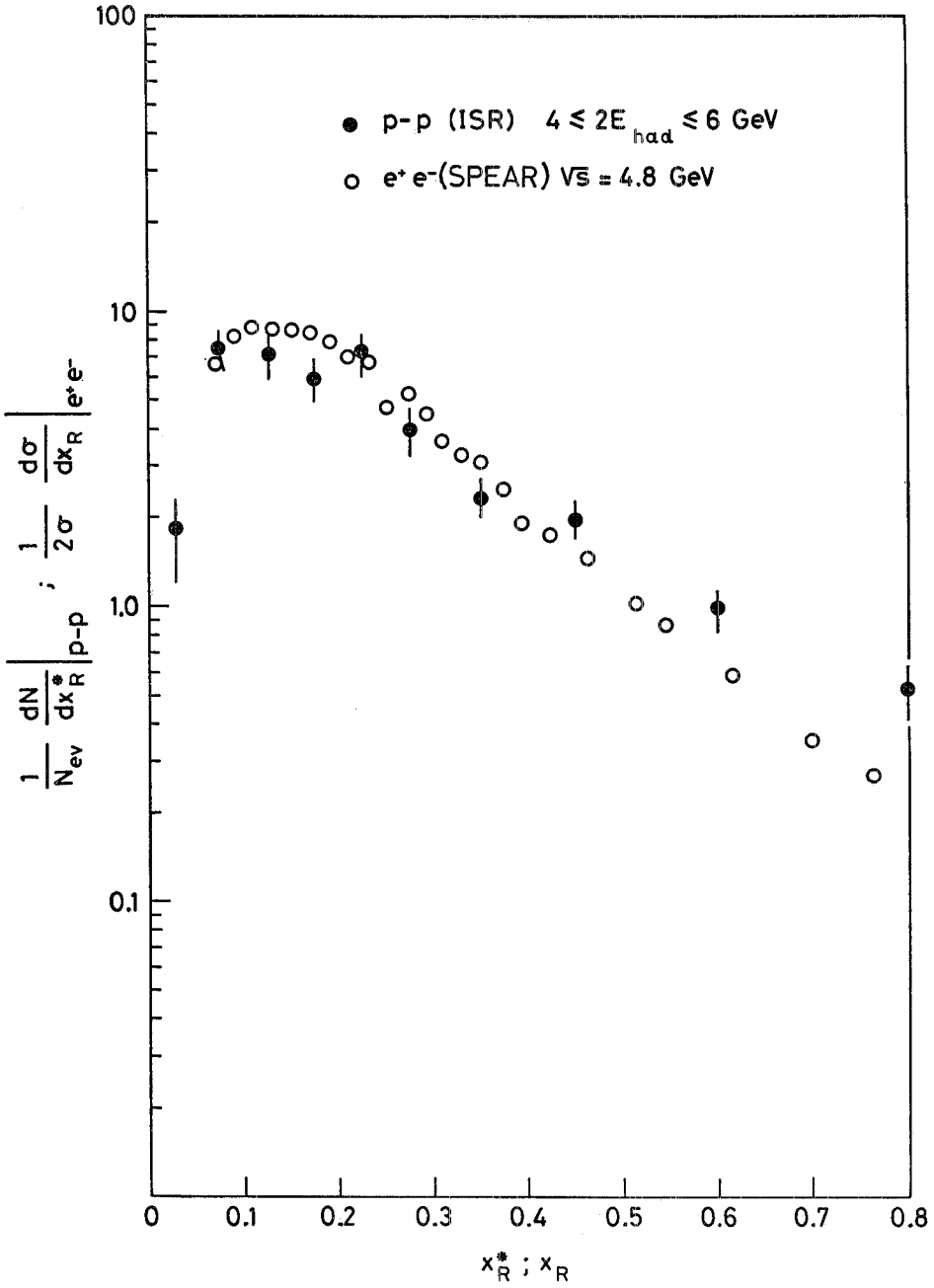

Fig. 5. – The inclusive single-particle fractional momentum distributions $(1/N_{ev})\cdot(dN/dx_R^*)$ in the interval 4 GeV $\leqslant 2E^{had} \leqslant$ 6 GeV obtained from data at $\sqrt{s} = 30$ GeV. Also shown are data from MARK I at SPEAR.

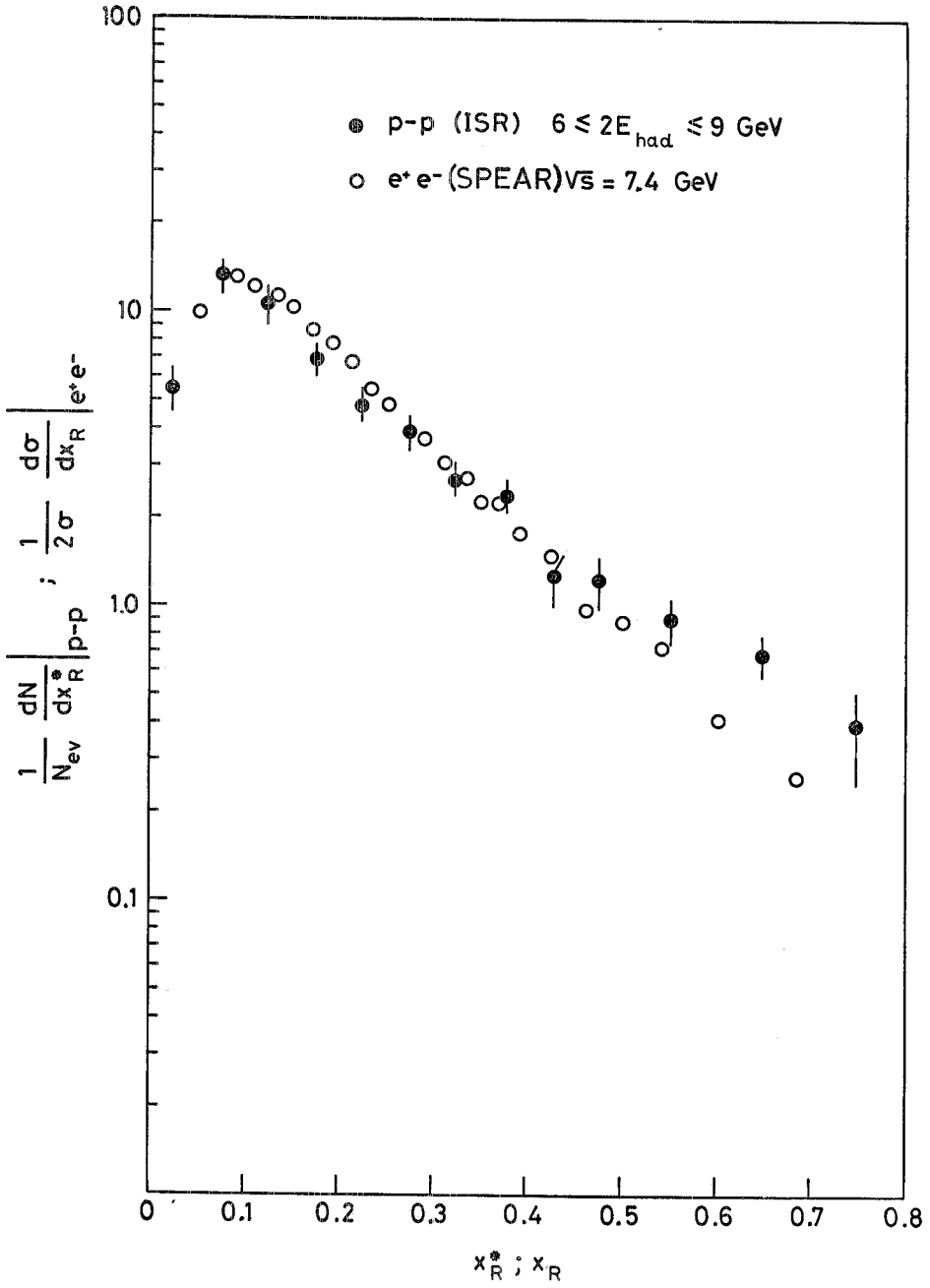

Fig. 6. – The inclusive single-particle fractional momentum distributions $(1/N_{cv})\cdot(dN/dx_R^*)$ in the interval 6 GeV $\leqslant 2E^{had} \leqslant$ 9 GeV obtained from data at $\sqrt{s} = 30$ GeV. Also shown are data from MARK I at SPEAR.

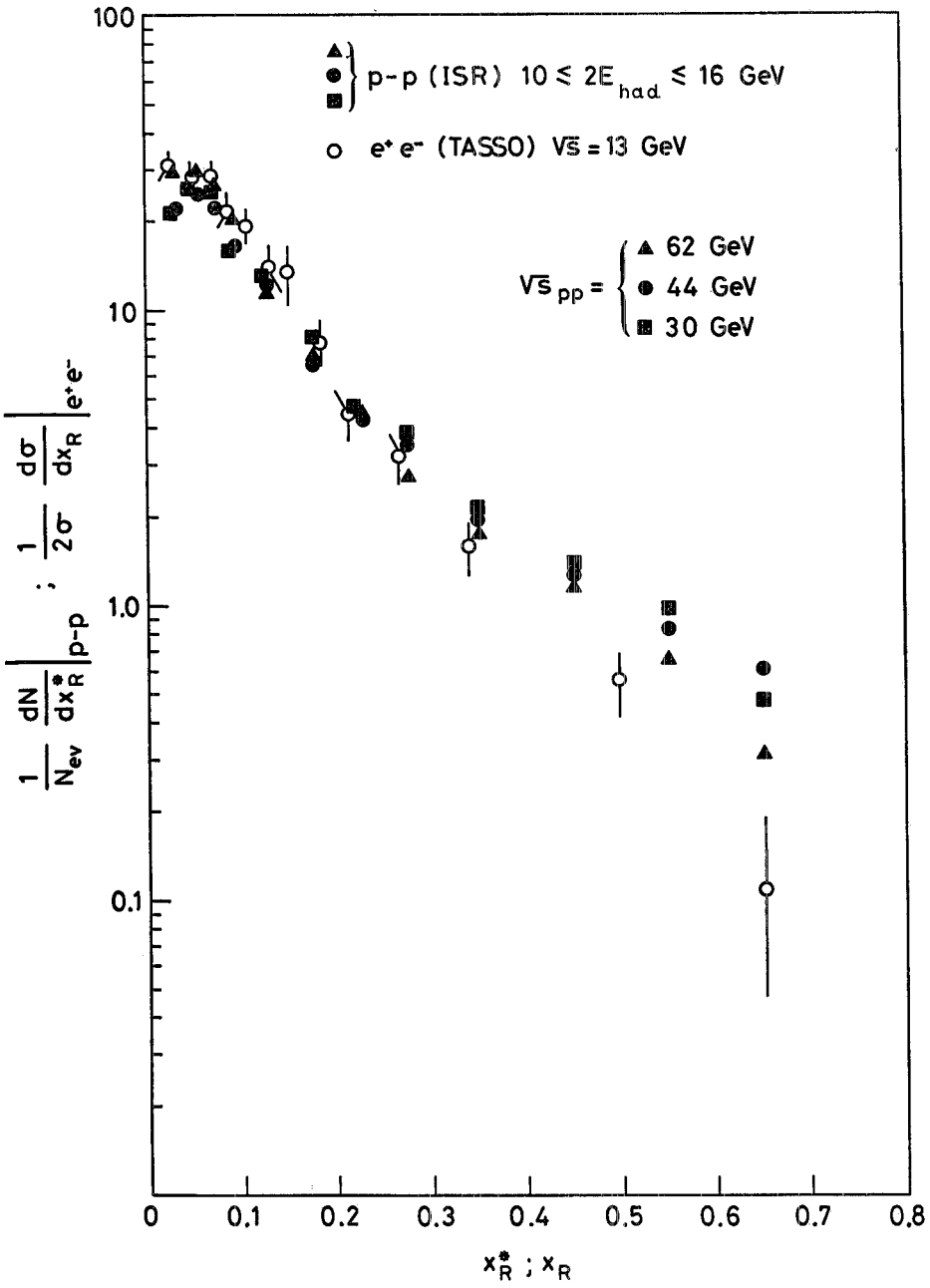

Fig. 7. – The inclusive single-particle fractional momentum distributions $(1/N_{ev})\cdot(\mathrm{d}N/\mathrm{d}x_R^*)$ in the interval $10\ \mathrm{GeV} \leqslant 2E^{had} \leqslant 16\ \mathrm{GeV}$ obtained from data at different $(\sqrt{s})_{pp}$. Also shown are data from TASSO at PETRA.

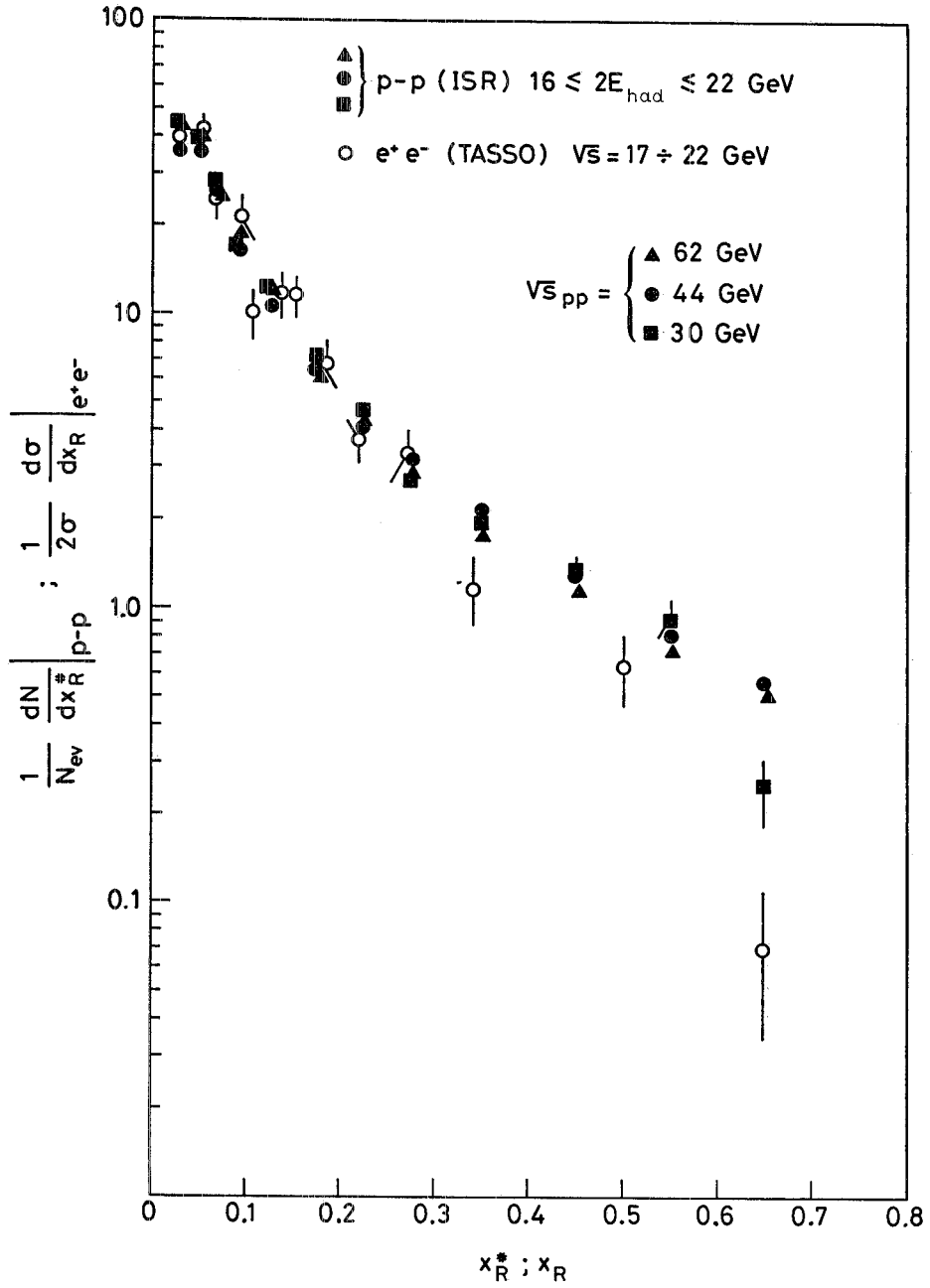

Fig. 8. – The inclusive single-particle fractional momentum distributions $(1/N_{ev})\cdot(dN/dx_R^*)$ in the interval $16\ \mathrm{GeV} \leqslant 2E^{had} \leqslant 22\ \mathrm{GeV}$ obtained from data at different $(\sqrt{s})_{pp}$. Also shown are data from TASSO at PETRA.

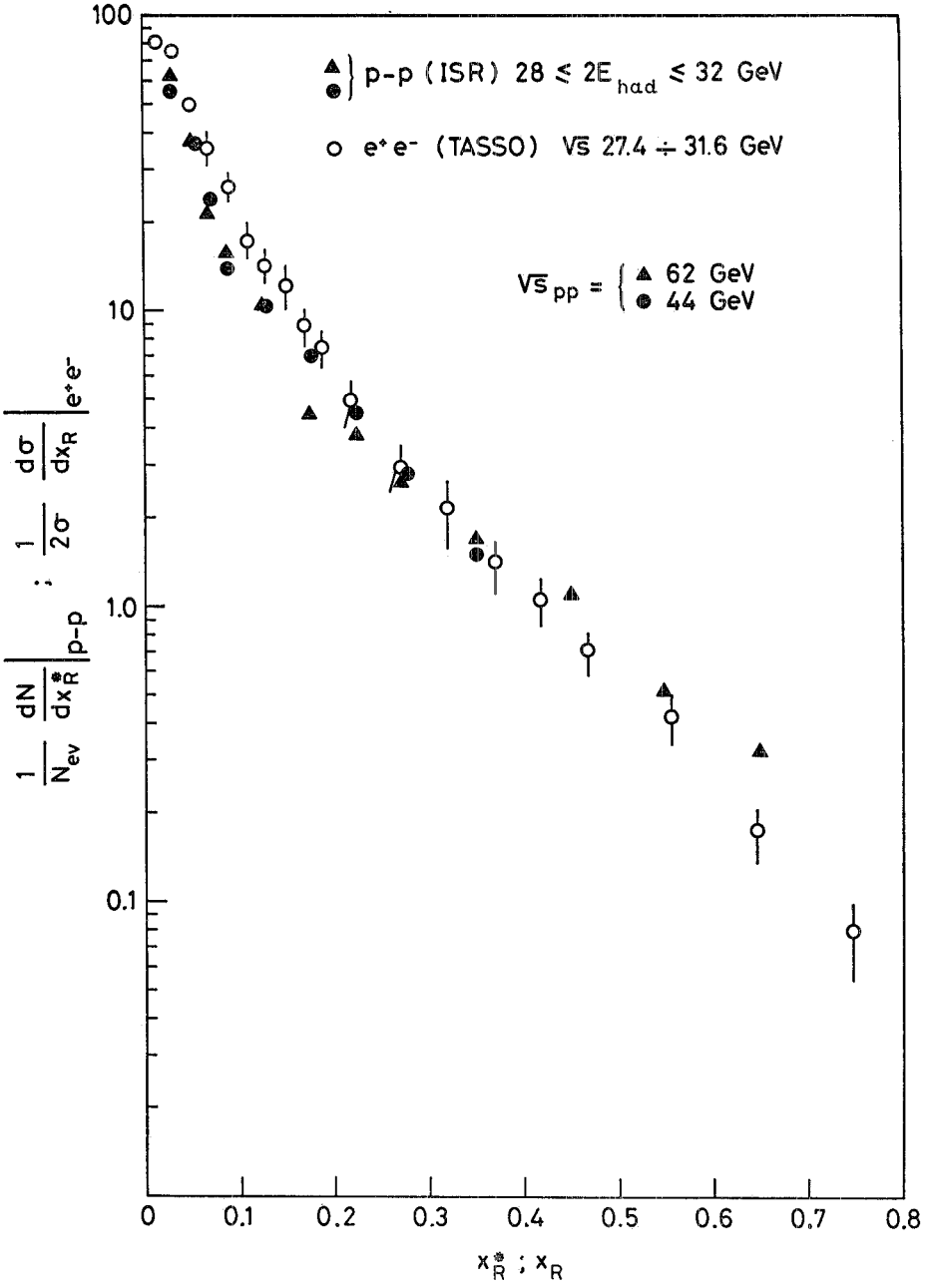

Fig. 9. – The inclusive single-particle fractional momentum distributions $(1/N_{ev})\cdot(dN/dx_R^*)$ in the interval 28 GeV $\leqslant 2E^{had} \leqslant$ 32 GeV obtained from data at different $(\sqrt{s})_{pp}$. Also shown are data from TASSO at PETRA.

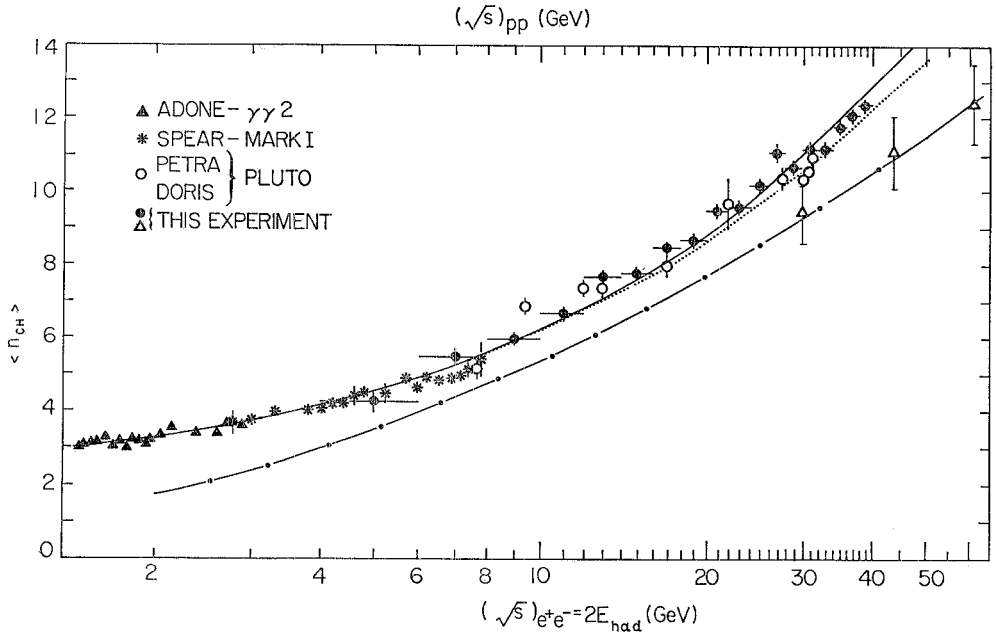

Fig. 10. – Mean charged-particle multiplicity (averaged over different $(\sqrt{s})_{pp}$) *vs.* $2E^{had}$, compared with (e^+e^-) data. The continuous line is the best fit to our data according to the formula $\langle n_{ch} \rangle = a + b \exp[c\sqrt{\ln (s/\Lambda)^2}]$. The dotted line is the best fit using PLUTO data. The dash-dotted line is the standard (pp) total charged-particle multiplicity with, superimposed, our data as open triangular points.

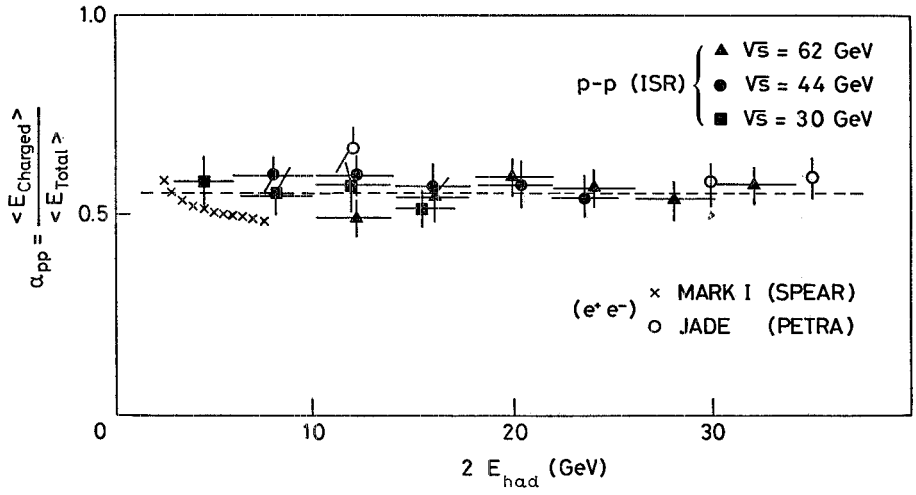

Fig. 11. – The charged-to-total energy ratio obtained in (pp) collisions α_{pp}, plotted *vs.* $2E^{had}$ and compared with (e^+e^-) obtained at SPEAR and PETRA.

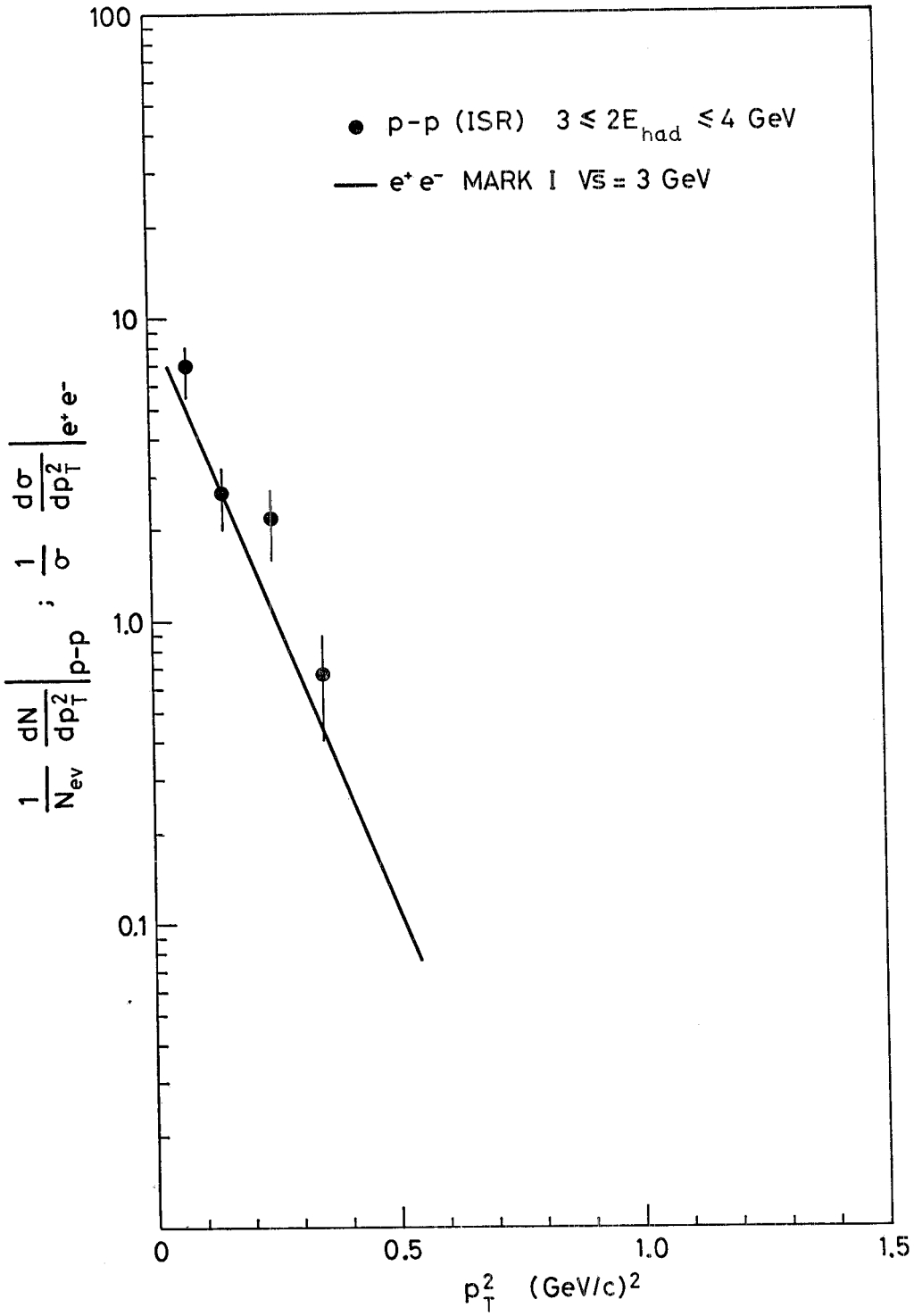

Fig. 12. – The inclusive single-particle transverse momentum distribution $(1/N_{ev})\cdot(dN/dp_T^2)$ in the interval $3\ \mathrm{GeV} \leqslant 2E^{had} \leqslant 4\ \mathrm{GeV}$ obtained from data at $\sqrt{s} = 30$ GeV. Also shown is the fit to the SPEAR data (continuous line).

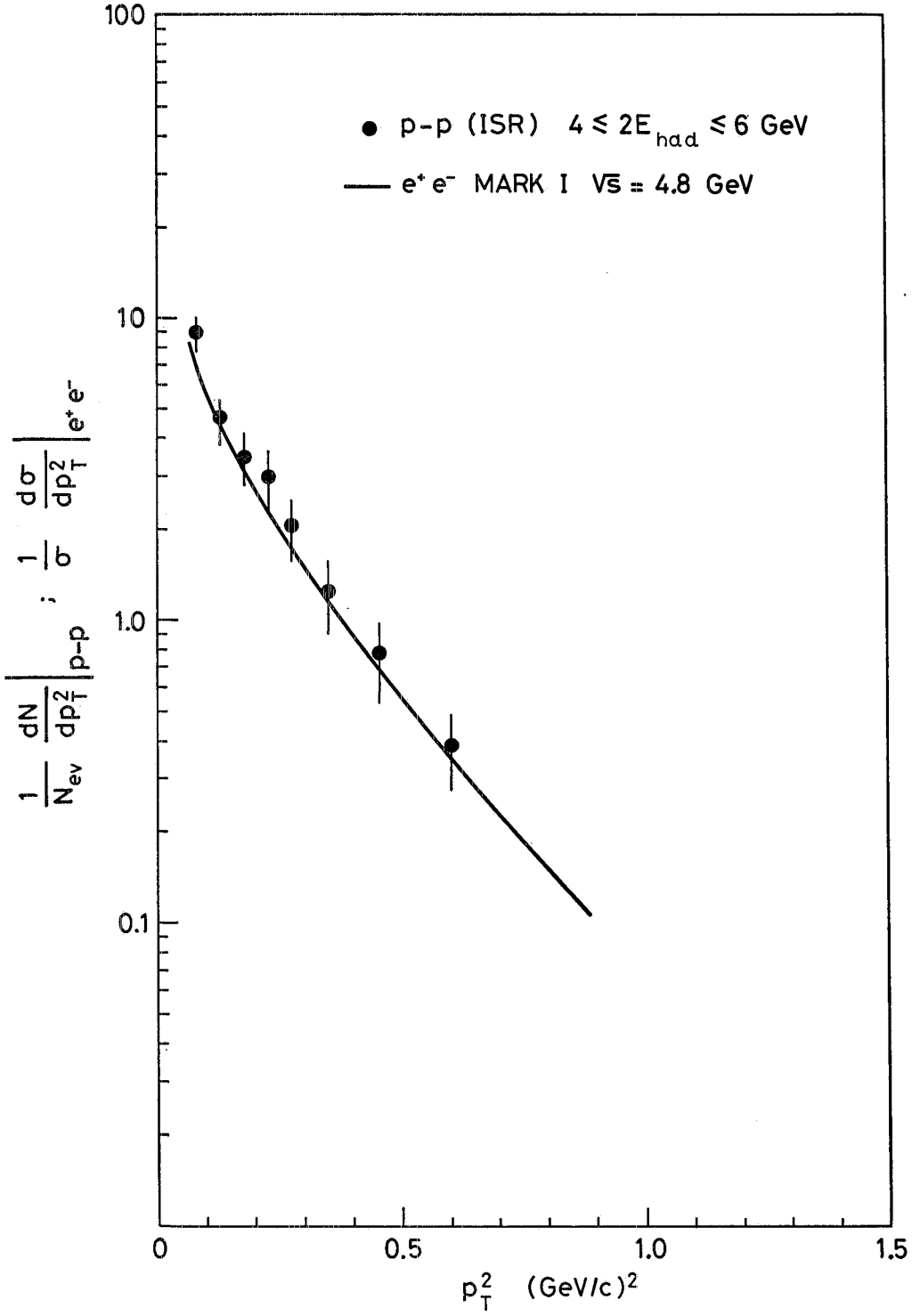

Fig. 13. – The inclusive single-particle transverse-momentum distribution $(1/N_{ev})\cdot(dN/dp_T^2)$ in the interval $4\ \mathrm{GeV} \leqslant 2E^{had} \leqslant 6\ \mathrm{GeV}$ obtained from data at $\sqrt{s} = 30$ GeV. Also shown is the fit to the SPEAR data (continuous line).

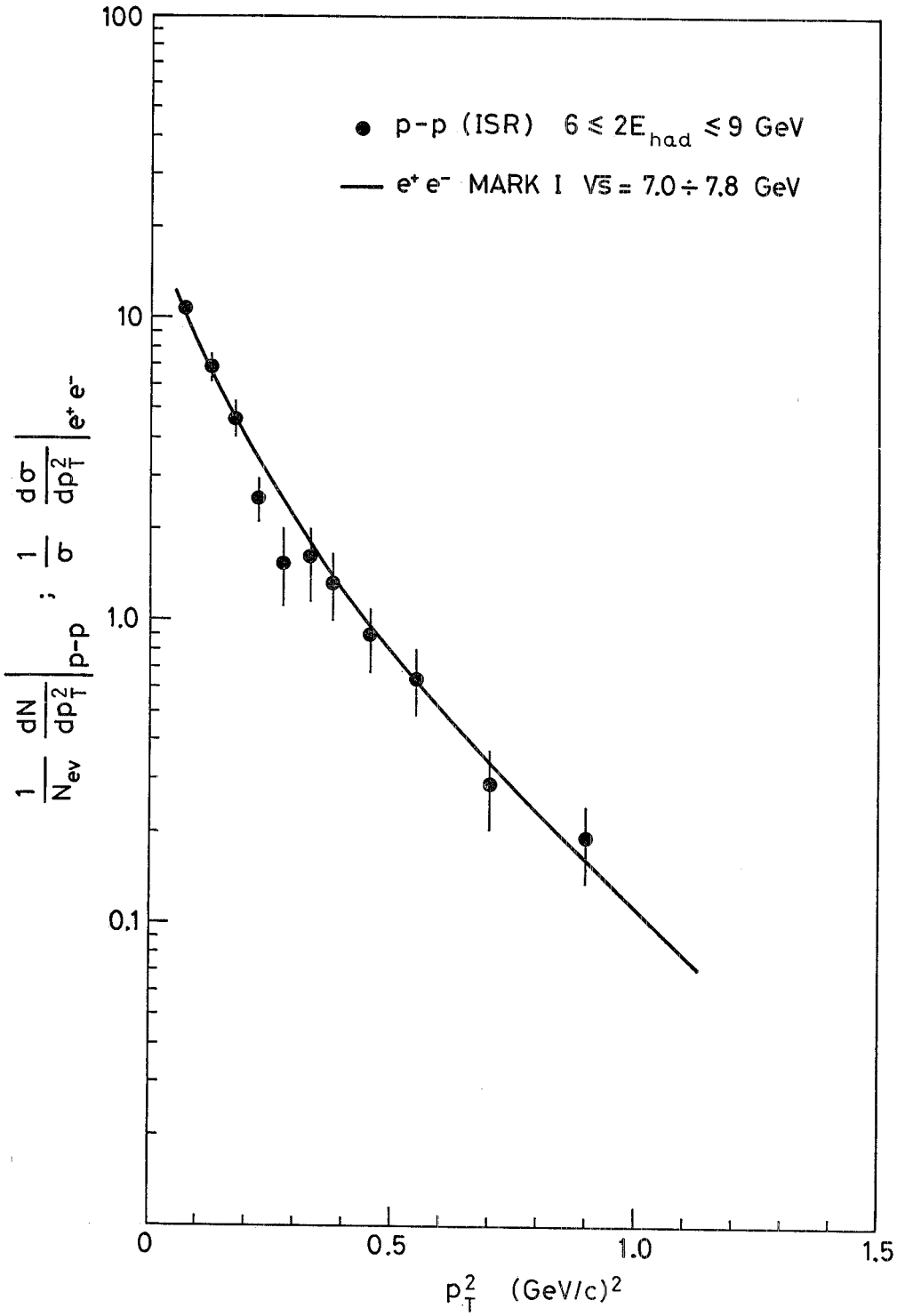

Fig. 14. – The inclusive single-particle transverse-momentum distribution $(1/N_{ev})\cdot(dN/dp_T^2)$ in the interval $6\ \text{GeV} \leqslant 2E^{had} \leqslant 9\ \text{GeV}$ obtained from data at $\sqrt{s} = 30\ \text{GeV}$. Also shown is the fit to the SPEAR data (continuous line).

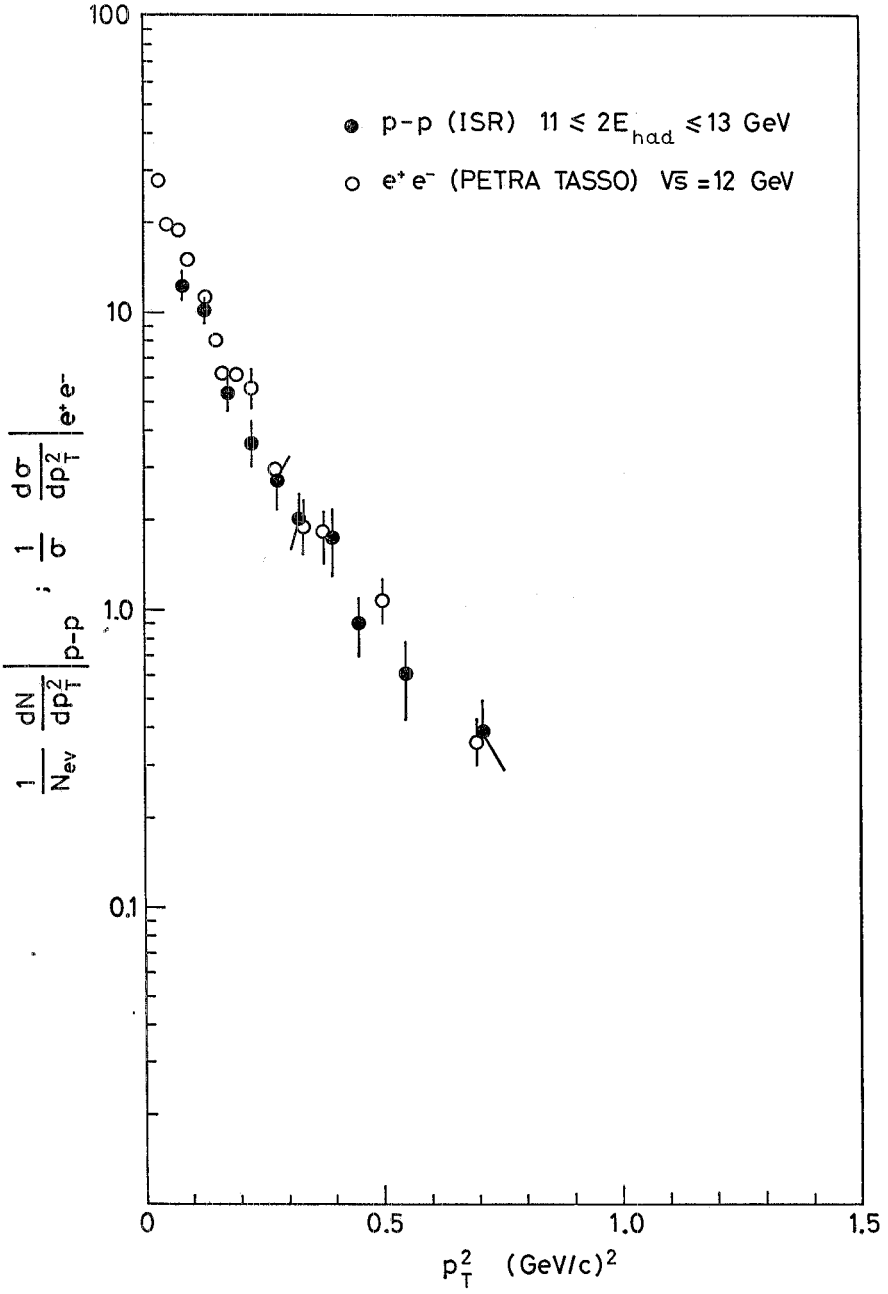

Fig. 15. – The inclusive single-particle transverse-momentum distributions $(1/N_{ev})\cdot(\mathrm{d}N/\mathrm{d}p_T^2)$ in the interval 11 GeV $\leqslant 2E^{had} \leqslant$ 13 GeV obtained from data at $\sqrt{s} = 62$ GeV. Also shown are data from TASSO at PETRA.

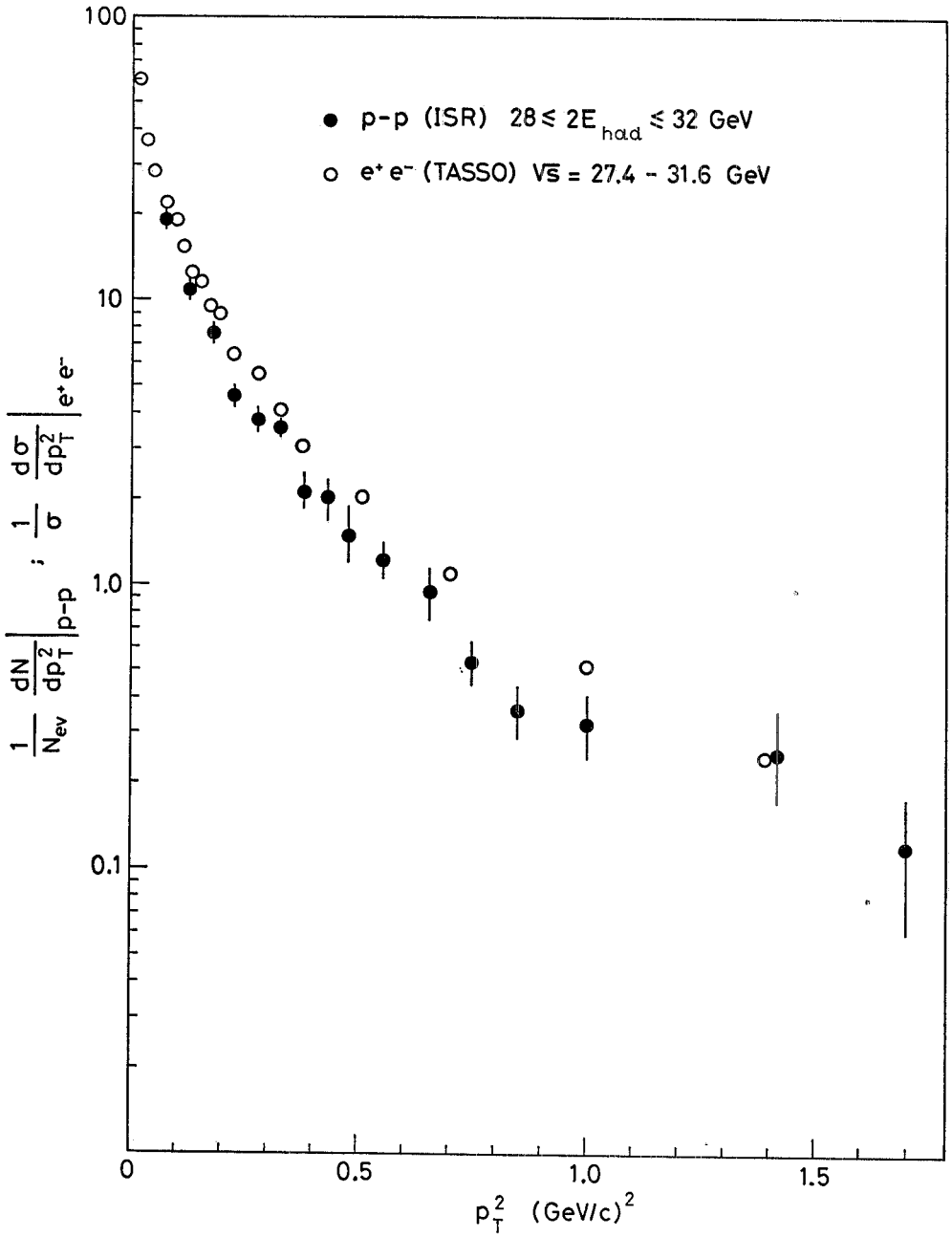

Fig. 16. – The inclusive single-particle transverse-momentum distributions $(1/N_{ev})\cdot(dN/dp_T^2)$ in the interval 28 GeV $\leqslant 2E^{had} \leqslant$ 32 GeV obtained from data at $\sqrt{s} = 62$ GeV Also shown are data from TASSO at PETRA.

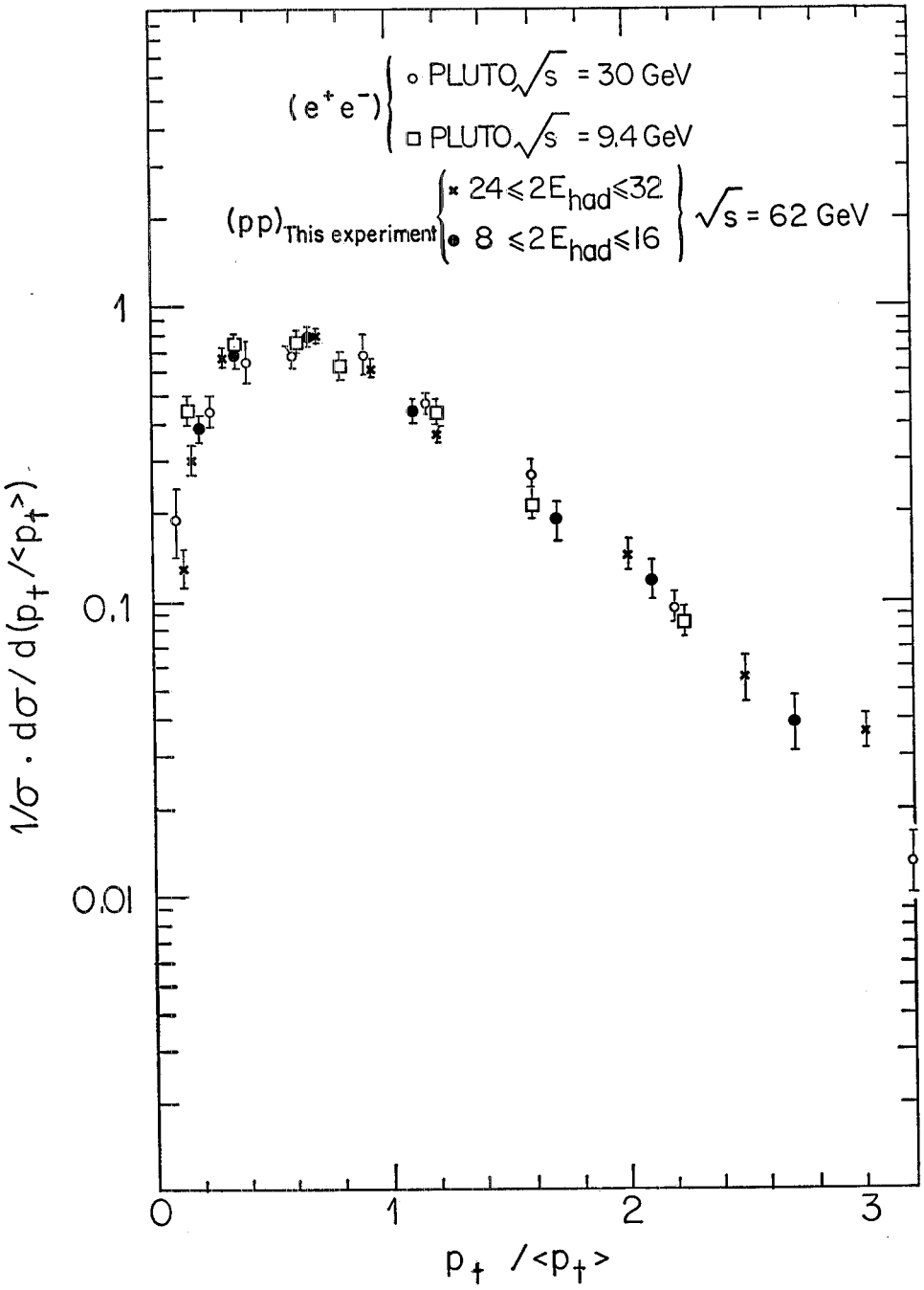

Fig. 17. – The differential cross-section $(1/\sigma)[d\sigma/d(p_t/\langle p_t\rangle)]$ *vs.* the « reduced » variable $p_t/\langle p_t\rangle$. These distributions allow a comparison of the multiparticle systems produced in (e^+e^-) annihilation and in (pp) interactions in terms of the renormalized transverse-momentum properties.

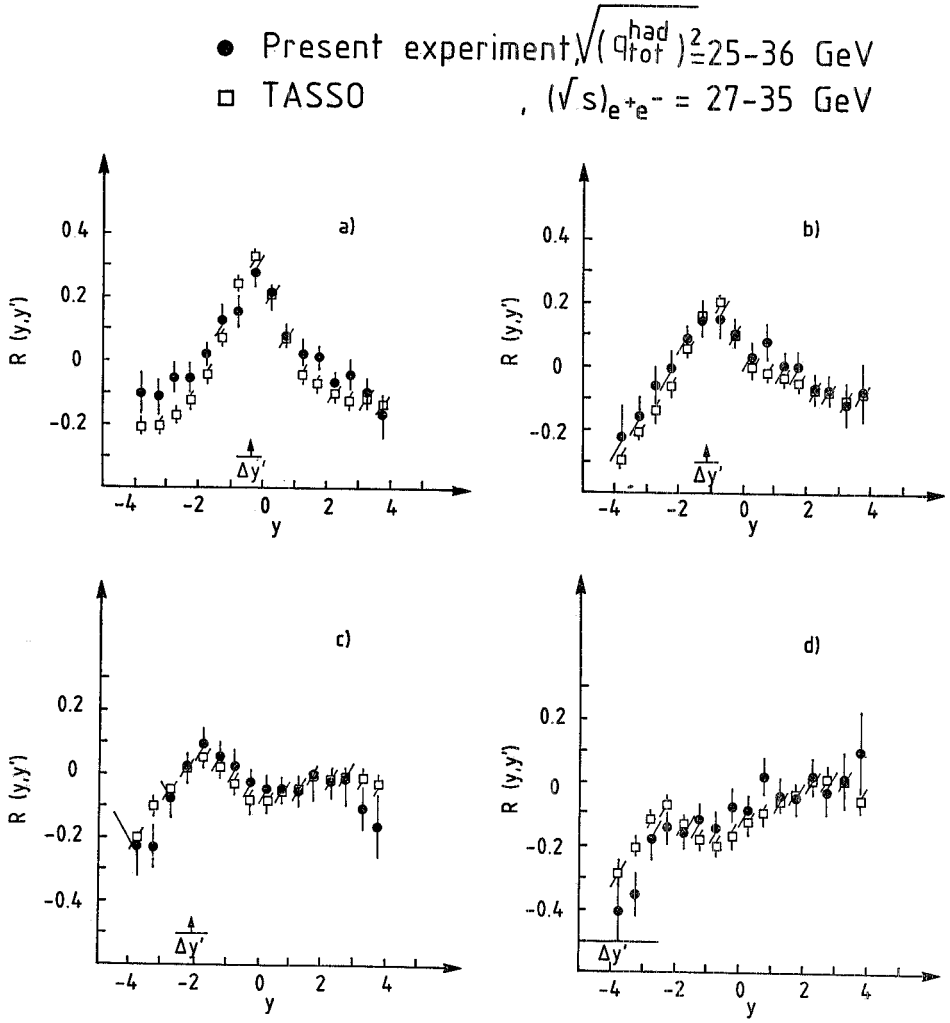

Fig. 18. – Two-particle correlation in rapidity space: $R(y, y')$, for different y' intervals, as measured in the present experiment after the leading-proton subtraction in the $\sqrt{(q_{tot}^{had})^2}$ range 25 to 36 GeV (black points), compared with the results by the TASSO collaboration at $(\sqrt{s})_{e^+e^-}$ between 27 and 35 GeV (open squares).

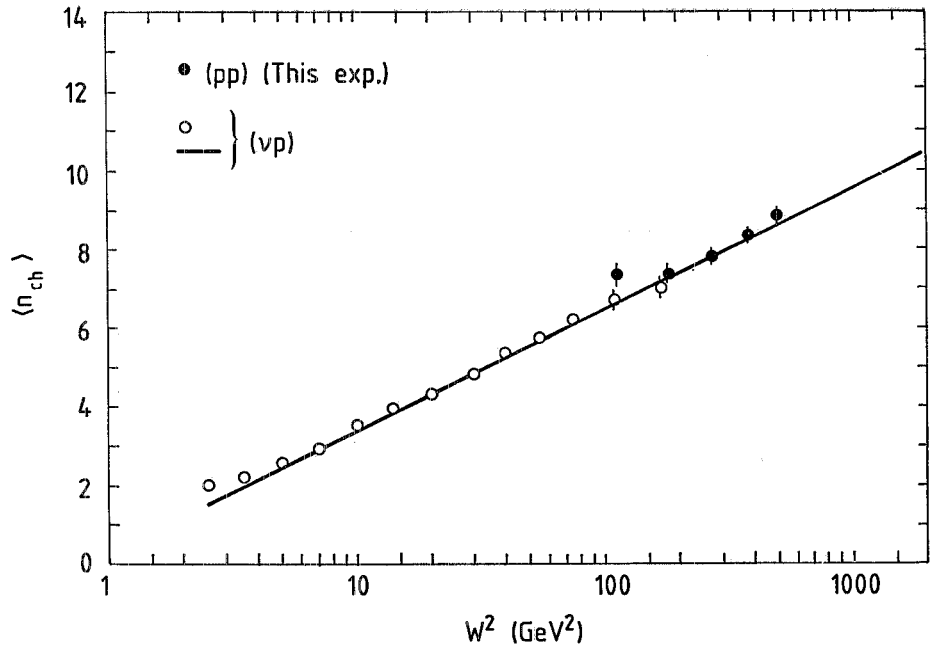

Fig. 19. – The average charged-particle multiplicities $\langle n_{ch} \rangle$ measured in (pp) at $(\sqrt{s})_{pp} = 30$ GeV, using a DIS-like analysis, are plotted *vs.* W^2 (black points). The open points are the (νp) data and the continuous line is their best fit.

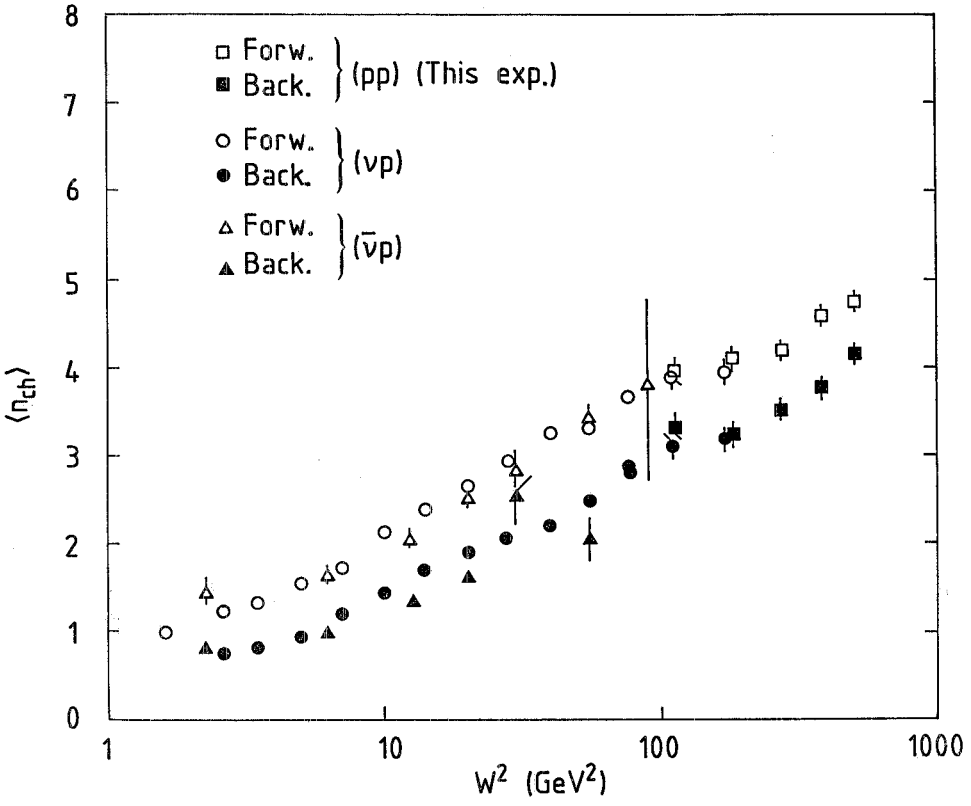

Fig. 20. – The mean charged-particle multiplicities $\langle n_{ch} \rangle_{F,B}$ in the forward and backward hemispheres *vs.* W^2, in (νp), ($\bar{\nu}$p) and (pp) interactions.

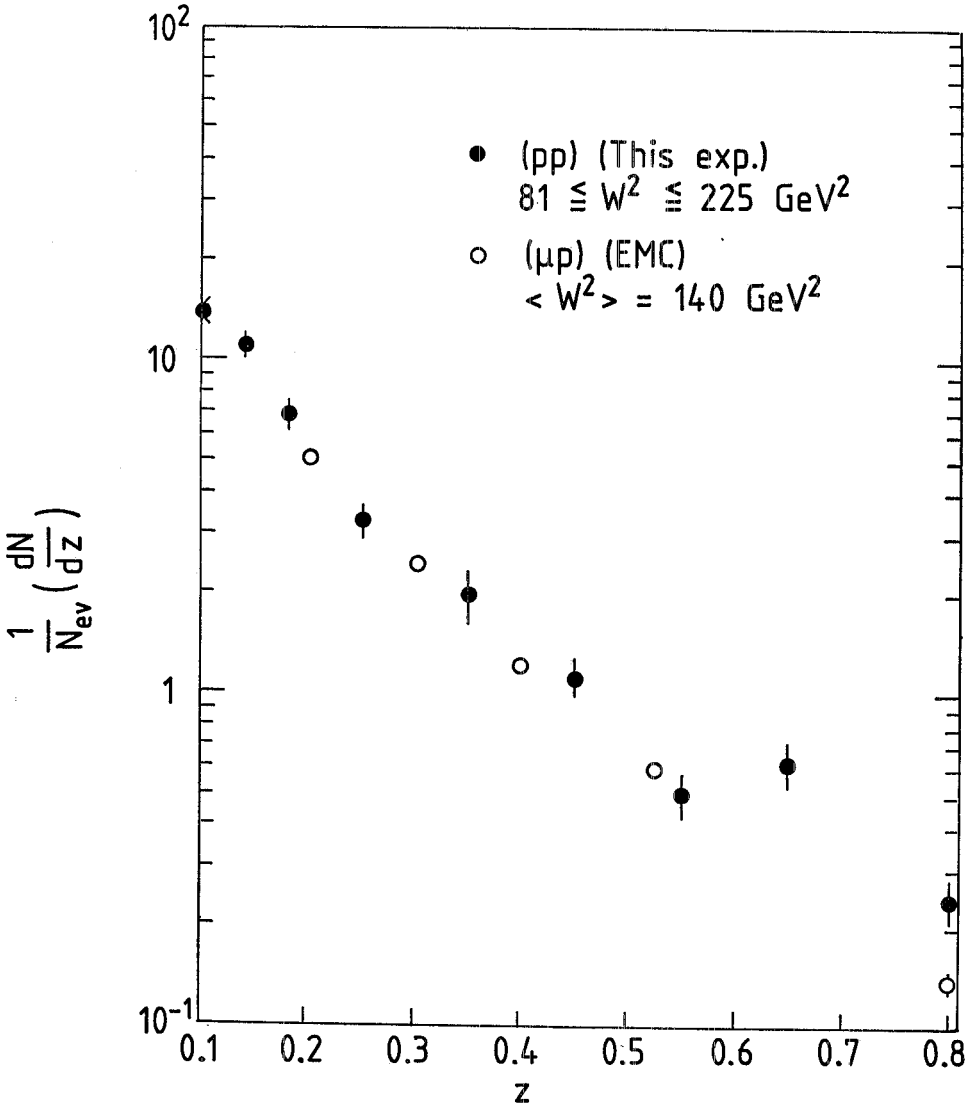

Fig. 21. – The inclusive distribution of the fractional energy z for (pp) reactions in the energy interval 81 $(\mathrm{GeV})^2 \leqslant W^2 \leqslant 225$ $(\mathrm{GeV})^2$ compared with the data from (μp) reactions at $\langle W^2 \rangle = 140$ $(\mathrm{GeV})^2$.

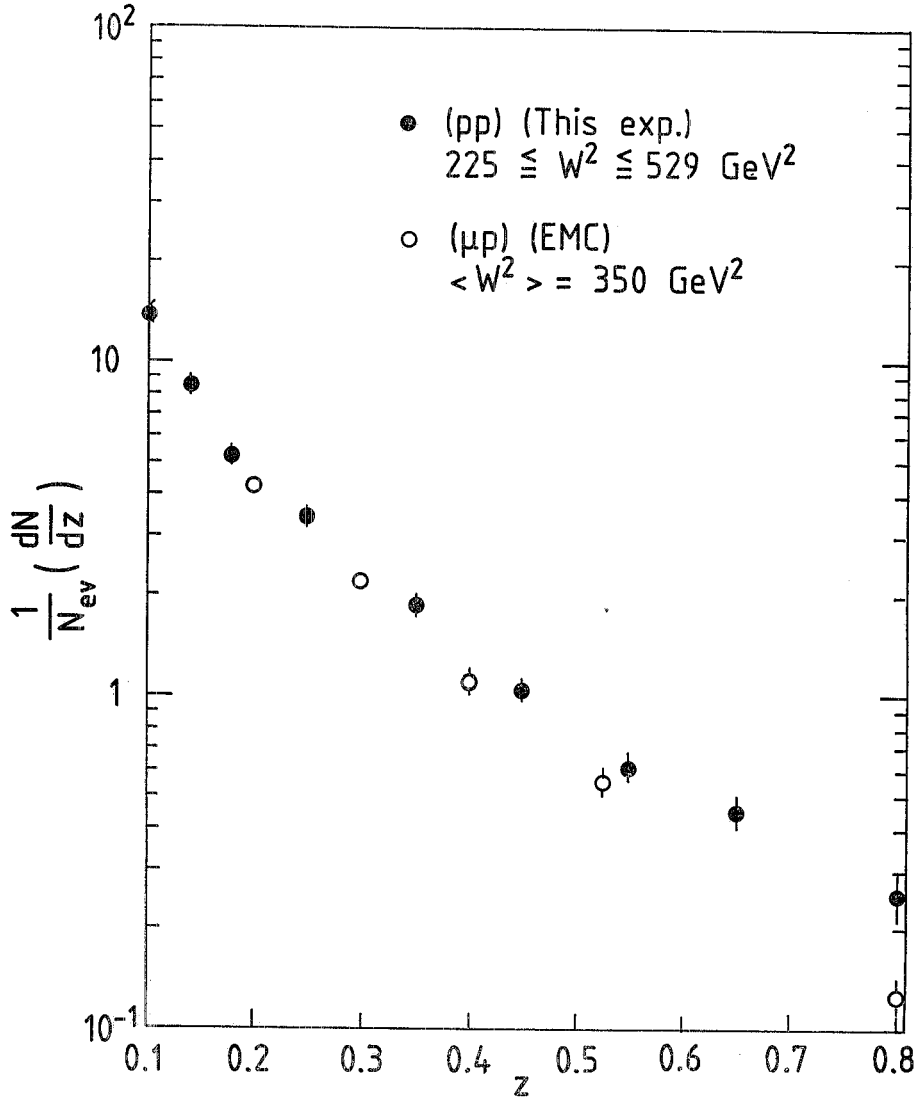

Fig. 22. – The inclusive distribution of the fractional energy z for (pp) reactions in the energy interval 225 $(\mathrm{GeV})^2 \leqslant W^2 \leqslant 529$ $(\mathrm{GeV})^2$, compared with the data from (μp) reactions at $\langle W^2 \rangle = 350$ $(\mathrm{GeV})^2$.

The experimental data in which (pp) interactions are compared with DIS are shown in fig. 19-22 and ref. [15-17].

These comparisons show striking analogies with respect to the following quantities:

i) the inclusive fractional energy distribution of the produced particles [1,2,9,11] (see fig. 4-9, 21, 22);

ii) the average charged-particle multiplicities [3,8,12,15,16] (see fig. 10, 19, 20);

B. ESPOSITO, P. GIUSTI, T. MASSAM, R. NANIA, F. PALMONARI, G. SARTORELLI, M. SPINETTI, G. SUSINNO, G. VALENTI, L. VOTANO and A. ZICHICHI: *Lett. Nuovo Cimento*, **31**, 273 (1981).

[8] M. BASILE, G. CARA ROMEO, L. CIFARELLI, A. CONTIN, G. D'ALÍ, P. DI CESARE, B. ESPOSITO, P. GIUSTI, T. MASSAM, R. NANIA, F. PALMONARI, V. ROSSI, G. SARTORELLI, M. SPINETTI, G. SUSINNO, G. VALENTI, L. VOTANO and A. ZICHICHI: *Nuovo Cimento A*, **65**, 400 (1981).

[9] M. BASILE, G. CARA ROMEO, L. CIFARELLI, A. CONTIN, G. D'ALÍ, P. DI CESARE, B. ESPOSITO, P. GIUSTI, T. MASSAM, R. NANIA, F. PALMONARI, V. ROSSI, G. SARTORELLI, M. SPINETTI, G. SUSINNO, G. VALENTI, L. VOTANO and A. ZICHICHI: *Nuovo Cimento A*, **65**, 414 (1981).

[10] M. BASILE, G. CARA ROMEO, L. CIFARELLI, A. CONTIN, G. D'ALÍ, P. DI CESARE, B. ESPOSITO, P. GIUSTI, T. MASSAM, R. NANIA, F. PALMONARI, V. ROSSI, G. SARTORELLI, M. SPINETTI, G. SUSINNO, G. VALENTI, L. VOTANO and A. ZICHICHI: *Lett. Nuovo Cimento*, **32**, 210 (1981).

[11] M. BASILE, G. CARA ROMEO, L. CIFARELLI, A. CONTIN, G. D'ALÍ, P. DI CESARE, B. ESPOSITO, P. GIUSTI, T. MASSAM, R. NANIA, F. PALMONARI, V. ROSSI, F. ROHRBACH, G. SARTORELLI, M. SPINETTI, G. SUSINNO, G. VALENTI, L. VOTANO and A. ZICHICHI: *Nuovo Cimento A*, **67**, 53 (1982).

[12] M. BASILE, G. BONVICINI, G. CARA ROMEO, L. CIFARELLI, A. CONTIN, M. CURATOLO, G. D'ALÍ, P. DI CESARE, B. ESPOSITO, P. GIUSTI, T. MASSAM, R. NANIA, F. PALMONARI, A. PETROSINO, V. ROSSI, G. SARTORELLI, M. SPINETTI, G. SUSINNO, G. VALENTI, L. VOTANO and A. ZICHICHI: *Nuovo Cimento A*, **67**, 244 (1982).

[13] M. BASILE, G. BONVICINI, G. CARA ROMEO, L. CIFARELLI, A. CONTIN, M. CURATOLO, G. D'ALÍ, C. DEL PAPA, B. ESPOSITO, P. GIUSTI, F. MASSAM, R. NANIA, F. PALMONARI, G. SARTORELLI, M. SPINETTI, G. SUSINNO, L. VOTANO and A. ZICHICHI: *Nuovo Cimento*, **73**, 329 (1983).

[14] G. BONVICINI, G. CARA ROMEO, L. CIFARELLI, A. CONTIN, M. CURATOLO, G. D'ALÍ, C. DEL PAPA, B. ESPOSITO, P. GIUSTI, T. MASSAM, R. NANIA, G. SARTORELLI, G. SUSINNO, L. VOTANO and A. ZICHICHI: *Lett. Nuovo Cimento*, **36**, 563 (1983).

[15] M. BASILE, G. BONVICINI, G. CARA ROMEO, L. CIFARELLI, A. CONTIN, M. CURATOLO, G. D'ALÍ, C. DEL PAPA, B. ESPOSITO, P. GIUSTI, T. MASSAM, R. NANIA, F. PALMONARI, G. SARTORELLI, G. SUSINNO, L. VOTANO and A. ZICHICHI: *Lett. Nuovo Cimento*, **36**, 303 (1983).

[16] G. BONVICINI, G. CARA ROMEO, L. CIFARELLI, A. CONTIN, M. CURATOLO, G. D'ALÍ, C. DEL PAPA, B. ESPOSITO, P. GIUSTI, T. MASSAM, R. NANIA, F. PALMONARI, G. SARTORELLI, G. SUSINNO, L. VOTANO and A. ZICHICHI: *Lett. Nuovo Cimento*, **36**, 555 (1983).

[17] G. BONVICINI, G. CARA ROMEO, L. CIFARELLI, A. CONTIN, M. CURATOLO, G. D'ALÍ, C. DEL PAPA, B. ESPOSITO, P. GIUSTI, T. MASSAM, R. NANIA, G. SARTORELLI, G. SUSINNO, L. VOTANO and A. ZICHICHI: *Lett. Nuovo Cimento*, **37**, 289 (1983).

iii) the ratio of the average energy associated with the charged particles over the total energy available for particle production ([5]) (see fig. 11);

iv) the inclusive transverse-momentum distribution of the produced particles ([7,10]) (see fig. 12-17);

v) the correlation functions in rapidity ([14]) (see fig. 18).

Notice the power of the (pp) interaction. Once this is analysed in the correct way, it produces results equivalent to (e^+e^-) and DIS.

This means that there is an important universality in these ways of producing multihadronic systems.

4. – Extrapolations to collider physics.

From the above analysis we can conclude that

i) the leading effects must be subtracted and the correct variables have to be used if we want to compare purely hadronic interactions with (e^+e^-) and DIS;

ii) the old myth, based on the belief that in order to compare (pp) with (e^+e^-) and DIS you need high-p_T (pp) interactions, is over. In fact we have proved that low-p_T (pp) interactions produce results in excellent agreement with (e^+e^-) annihilation and DIS processes, the basic parameter in (pp) interactions being $\sqrt{(q_{tot}^{had})^2}$ for a comparison with (e^+e^-), and $\sqrt{W^2_{(pp)}}$ for a comparison with DIS.

The existence of high-p_T events means that pointlike constituents exist inside the nucleon. But low-p_T events contain the same amount of basic information as high-p_T events. The only difference is expected in $\langle p_t \rangle$. In fact our analysis of the inclusive transverse-momentum distribution, in terms of the renormalized variable $p_t/\langle p_t \rangle$ (notice that p_t indicates the transverse momentum of the particles produced with respect to the jet axis, and p_T with respect to the colliding (pp) or ($p\bar{p}$) axis), is suggestive of a very interesting possibility: multiparticle systems produced at high p_T could show, at equivalent $\sqrt{(q_{tot}^{had})^2}$, higher values of $\langle p_t \rangle$. This should be the only difference between multiparticle systems with the same $\sqrt{(q_{tot}^{had})^2}$ produced at low p_T and high p_T.

There are two ways of producing $\sqrt{(q_{tot}^{had})^2}$:

i) one is at low p_T, and we have seen what happens;

ii) the other is at high p_T: we have not been able to compare, at constant values of $\sqrt{(q_{tot}^{had})^2}$, the multiparticle systems produced in (pp) interactions at high p_T and low p_T, the reason being the lack of CERN ISR time. However,

as mentioned above, the agreement between our data and (e^+e^-) data in the variable $(p_t/\langle p_t\rangle)$, makes it possible to foresee what should change between low-p_T and high-p_T multiparticle jets.

Now we come to the extrapolation: *the extrapolation of our method to the* CERN $p\bar{p}$ *collider* [18,19] would allow a large energy jump and could produce clear evidence for or against our prediction. For example, if two jets at the $p\bar{p}$ collider are produced back-to-back with the same transverse energy E_T, then we have

$$\sqrt{(q_{tot}^{had})^2} \simeq 2E_T .$$

Suppose that we are at

$$2E_T = 100 \text{ GeV} .$$

This system, according to our extrapolation, should be like a multiparticle state produced by $(\sqrt{s})_{e^+e^-} = 100$ GeV.

However, there is a very important check to make using collider data, without the need for the (e^+e^-) data.

The key point is to see if, at the CERN $p\bar{p}$ collider, a multiparticle system produced at low p_T but with

$$\sqrt{(q_{tot}^{had})^2} = 100 \text{ GeV}$$

looks like the one produced at high E_T. The main difference we can expect is the value of $\langle p_t\rangle$.

To check these points is another important contribution to understanding hadron production at extreme energies.

5. – Conclusions.

The new method of studying (pp) and $(p\bar{p})$ collisions—based on the subtraction of the « leading » effects and the use of correct variables—allows us to put on equal footing the multiparticle systems that are produced in purely hadronic interactions, in (e^+e^-) annihilation and in DIS processes.

The implications of this method for the physics to be studied in future machines are of great interest.

Purely hadronic interactions means using machines such as the CERN Intersecting Storage Ring (ISR), the CERN $p\bar{p}$ collider, the BNL-CBA collider, and the FNAL $p\bar{p}$ collider.

---

[18] UA2 Collaboration: *Phys. Lett. B*, **118**, 203 (1982).
[19] UA1 Collaboration: preprint CERN-EP/83-02 (1983).

(e^+e^-) *annihilation* means using machines such as LEP and its possible developments.

DIS *processes* means using machines such as HERA.

The « leading » subtraction and the use of the correct variables allow us to show that universality features are present, in the production of multibody final states in (pp), (e^+e^-) and DIS.

● RIASSUNTO

L'uso delle variabili corrette, nei processi (pp), (e^+e^-) e scattering inelastico profondo (DIS), permette di mettere in evidenza l'esistenza di caratteristiche universali in tali interazioni, considerate sinora modi molto differenti di produrre stati multiadronici.

Универсальные особенности в (pp), (e^+e^-) и процессах глубоко неупругого рассеяния.

Резюме (*). — Использование правильных переменных в (p, p), (e^+e^-) и процессах глубоко неупругого рассеяния позволяет установить универсальные особенности в этих реакциях.

(*) *Переведено редакцией.*